Available online at www.sciencedirect.com
SCIENCE DIRECT
ACADEMIC PRESS
Journal of Sound and Vibration 266 (2003) 655–665
JOURNAL OF SOUND AND VIBRATION
www.elsevier.com/locate/jsvi

First experiments on ultrasonic crop density measurement

K. Maertens*, P. Reyns, J. De Clippel, J. De Baerdemaeker

Laboratory for Agro-Machinery and Processing, Catholic University Leuven, Kasteelpark Arenberg 30, 3001 Leuven, Belgium

Received 13 January 2003

Abstract

An on-line crop density measurement delivers interesting information about the local crop condition. Once this measurement is established in a non-destructive way, crop density monitoring could be performed during the growing season and results would immediately be used for a site-specific application of nitrogen.

In this work, some primary results are shown from an ultrasonic crop density measurement. A commercial sensor, normally used for level measurements, is equipped with an extra output, providing a signal corresponding with the ultrasonic wave transmitted through a band of crop. Because of the properties of the measured signal, a non-linear transformation of the measured signal is necessary. With the result of this static compensation, a good estimation can be found of the energy in the received wave, closely related with the volumetric density of the crop.

Once the appropriate signal is found, an experimental set-up is constructed for dynamic crop density measurements. A small wagon is placed on two parallel rails with a stroke of crop in between. On both sides of this wagon, two ultrasonic transducers are placed. One as transmitter of the ultrasonic wave, the other one as receiver at the other side of the crop. With this arrangement, a first calibration curve is made, delivering an exponential relationship between the transmitted energy and volumetric crop density.

1. Introduction

Crop density (stems per square metre) is a factor which has an important influence on the crop condition during and after the growing season. This parameter immediately affects grain and straw yield but also determines the susceptibility for diseases and fungi.

When the plant population can be measured in a non-destructive way, useful information is available for applying site-specific fertilization doses. Studies have already shown the importance

*Corresponding author.
E-mail address: koen.maertens@agr.kuleuven.ac.be (K. Maertens).

0022-460X/$ - see front matter
doi:10.1016/S0022-460X(03)00591-1

of acquiring an optimal combination of nitrogen availability and crop density for maize [1]. Particularly, for low nitrogen availability, plant density has an important influence. The narrower the row spacing, the higher becomes the grain kernel number and grain yield, but higher risks appear for fungi and plant diseases. Similar studies have been performed on other types of crop [2,3].

Up to now, mapping of within-field variation of shoot density of wheat and barley at the beginning of the growing season is mostly carried out by means of optical measurements [4,5]. Reflectance of red and near-infrared wavelengths are measured optically and combined into a normalized difference vegetation index (NDVI) which is linearly correlated with shoot density. Image processing techniques for automatically counting plants are not established yet because of the overlapping of neighbouring plants.

Crop density measurements on a combine harvester at the time of harvesting were performed by Taylor et al. [6] by installing a laser beam in front of the header at the height of the cutterbar. The signal was used for an automatic speed control of the harvester. Other research [7] was based on a similar set-up, but using infrared light. Each interruption of the beam is counted. This value is divided by the width between transmitter and receiver and travel speed. The result is in counts per square metre and is considered as a measure for crop density. The results were promising for corn, but this was not the case for wheat. The maximum sample rate (800 Hz) was a limitation for high plant populations.

For haulm and stalky plant varieties, a measurement device and some first results for an indirect biomass sensors are presented in Ref. [8]. The measurement tool consists of a pendulum that is guided across a standing plant population. In the case of high local biomasses, the pendulum will be pushed more backwards and the measured angle with the vertical direction will increase. An analogous methodology is applied by De Clippel [9]. In the latter study, a curved plate is pulled over the standing crop and the force reaction is linked with the local biomass. Both measurements give only a rough indication of the actual biomass since they are strongly influenced by the physical properties of the standing crop.

In this work, a method is investigated, based on ultrasonic transducers. Within the framework of precision farming, ultrasonic distance sensors are installed on both sides of the cutterbar for measuring the actual cutting width during harvest [10]. When the same sensors could be used as crop density measurement, new information can be achieved with no need of extra space or instruments. Here the electronic circuit of cutting width sensors is analyzed, the appropriate signal is chosen corresponding with the received ultrasonic wave. Afterwards, primary results are shown from an experimental set-up where the conditions during harvest can be simulated in a dynamic way. Those results are based upon attenuation of ultrasonic waves transmitted through a stripe of wheat plants with different densities.

2. Materials and methods

A straightforward method for measuring the volumetric crop density between two points is to send an acoustic or electromagnetic wave with known energy level and to measure the transmitted energy at the other side of the crop. The lost energy will be correlated with the amount of stems in between and by this the plant population. The degree of attenuation will be directly determined by the wave frequency and radius of the stems. The basic phenomenon behind this attenuation is diffraction. The smaller the wavelength compared with the dimension of the obstacle, the more obvious diffraction will play its role. For wheat stems with a diameter of 5 mm and a wave speed of 330 m/s the transition frequency for diffraction lays at about 66 kHz, close to the working region of commercial ultrasonic distance sensors.

2.1. Ultrasonic transducer

As an ultrasonic transducer, a commercial sensor for level measurements has been used (Field 30 series Usonar Bin Sensor). Fig. 1 shows the basic electronic circuit.

2.1.1. Standard operation

An ultrasonic sensor for distance measurements works both as transmitter and receiver of the ultrasonic wave. First the electronic circuit will generate a burst and the membrane converts it into an ultrasonic wave. Next, the same membrane receives a certain reflection of the wave. A signal conditioning circuit processes the corresponding signal and delivers a value proportional to the time difference between sending and receiving.

2.1.1.1. Transmitter. As a signal for distance measurements, a burst composed of 50 and 60 kHz frequency components is applied for assuring an optimal surface detection. This signal enters the circuit (Fig. 1) via an MPSA13-transistor (Q_1). The transistor works as a switch and pulls a current burst through the primary of the transformer T_1. This transformer, with ratio 40, converts the 5 V signal into a high-voltage burst. Two 1N5281 zener diodes Z_1 and Z_2 are protecting the membrane Us from high-voltage peaks. The capacitor C_1 removes the low-frequency part from the signal. By this means, signal V_s consists of a high-frequency burst with a zero mean value and limited absolute voltage ($< \pm 100$ V). Membrane Us converts this voltage signal into an ultrasonic wave.

2.1.1.2. Receiver. When the ultrasonic transducer receives an acoustic wave, Us transforms it into an electric load. This load is discharged via two high-speed 1N4148 diodes D_1 and D_2, capacitance C_1 and the secondary transformer T_1. Voltage V_D across these anti-parallel diodes is subsequently amplified, filtered and integrated. Finally, a *Schmitt trigger* circuit is installed as indication for the wave arrival. The same microprocessor as for generating the output burst is used for converting

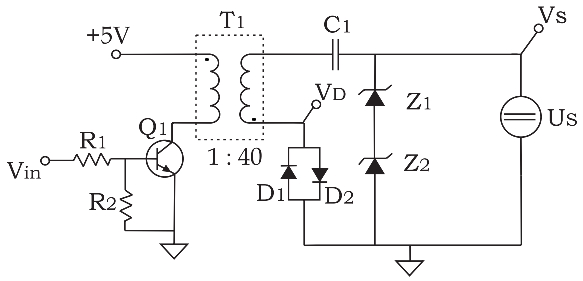

Fig. 1. Basic electronic circuit of ultrasonic sensor: V_{in}, input signal from signal generator; V_s, voltage on ultrasonic transducer and V_D, output signal across anti-parallel, high-speed diodes.

this indication signal into an analogue signal, proportional to the time delay between emission and receipt of the ultrasonic wave.

2.1.2. Relation between V_D and V_s

The non-linear current–voltage characteristic ($I_D = f_D(V_D)$) of D_1 and D_2 plays an essential role for detecting high-frequency content in V_s. A good approximation of this characteristic is given by (see Fig. 2)

$$I_D = \begin{cases} 0.383 \times 10^{-11}(\exp^{28.512 V_D} - 1) & (V_D \leqslant 0.79) \\ 0.0507 \exp^{2.086 V_D} - 0.2396 & (V_D > 0.79). \end{cases} \tag{1}$$

The different parameters are estimated based on specifications given by the technical datasheet of the high-speed diode. The estimation of the different parameters is a non-convex optimization problem. A global minimum if found by using the *Nelder–Mead Simplex Method* [11]. The advantage of this non-linearity for distance measurements is double:

- Low currents I_D (<10 mA) through the secondary of transformer T_1 result in relatively high V_D-values. This latter Property makes it easier to detect small current perturbations.
- The energy of the received burst will be depending on the measured distance. Longer distances will result in lower currents. The steep exponential curves at both sides of Fig. 2 brings these currents back to a more or less constant voltage space ($-0.8 < V_D < +0.8$) for a whole range of distances.

Both properties are interesting with respect to detection of high frequencies, but are not feasible for estimating the energy level of the ultrasonic wave. A non-linear compensation must be introduced for estimating the amplitude of V_s by measuring V_D.

Note that it is impossible to measure V_s directly. Because of the high output impedance of membrane U_s, measuring V_s needs an instrument with a high input impedance. When this impedance is too low, the current for discharging U_s will follow the instrument instead of diodes

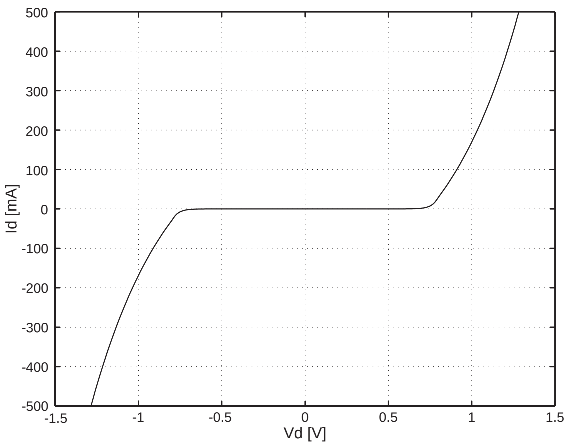

Fig. 2. Static characteristic $I_D = f_D(V_D)$ of two anti-parallel, 1N4148 high-speed diodes.

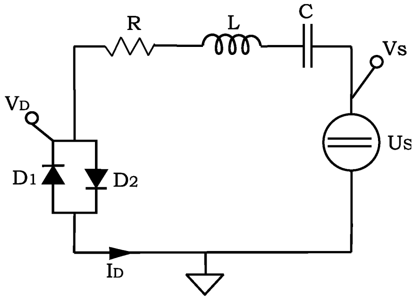

Fig. 3. Simplified secondary loop of transformer T_1.

D_1 and D_2. Experiments showed how even the influence of a high impedance oscilloscope (> 10 MΩ) deteriorates the distance measurement significantly.

When no input signal V_{in} is applied and no high-voltage peaks are present (Z_1 and Z_2 can be neglected for normal working conditions), the electronic circuit of Fig. 1 can be simplified into the schematics of Fig. 3. This simplified scheme results in the following non-linear differential equation, expressing the dynamic relationship between the actual voltage V_s across membrane Us and the measurable voltage V_D across the anti-parallel diodes:

$$V_D + \left(R + sL + \frac{1}{sC}\right) f_D(V_D) = V_s \qquad (2)$$

with s being the *Laplace* operator; R the resistance of the secondary spool of transformer T_1 (188 Ω); L the line and mutual inductance of the secondary spool of T_1 (21 mH); C the capacitance of C_1 (10^{-9} F).

Eq. (2) gives the possibility for transforming V_D-measurements into a V_s-estimation. To calculate the inverse dynamic relation is difficult since a good approximation of $f_D^{-1}(I_D)$ is not possible by means of a combination of some simple mathematical functions (1). Fig. 4 shows an example of signal reconstruction. As input V_D of Eq. (2), a 45 kHz sine of 0.525 V is applied. The corresponding voltage band lies mainly in the linear part of the diodes. The peaks in the current I_D correspond with the beginning of the non-linearity. Subsequently, these current peaks result in voltage peaks on the estimated V_s. The high discrepancy between both signals illustrates the importance of a compensation for estimating V_s.

2.2. Experimental set-up

Fig. 5 shows the 10 m experimental set-up for dynamic measurements. Three rows of wheat plants are placed in a sand box with metal grid. The length is divided in six sections with five different crop densities (Fig. 6). In two sections, a crop density of 367 stems/m^2 is planted. One section contains only half as much planted rows as the second one, but with a double density of stems in one row. Two rails are placed on both sides of the box, 1 m above the ground. A four-wheel cart is placed on both rails and pulled by an electrical motor (ELECTRAMO, model DE 90L). This motor is controlled by a PWM-inverter (T-verter, model N2-203-M), generating a cart speed between 0.1 and 1.25 m/s.

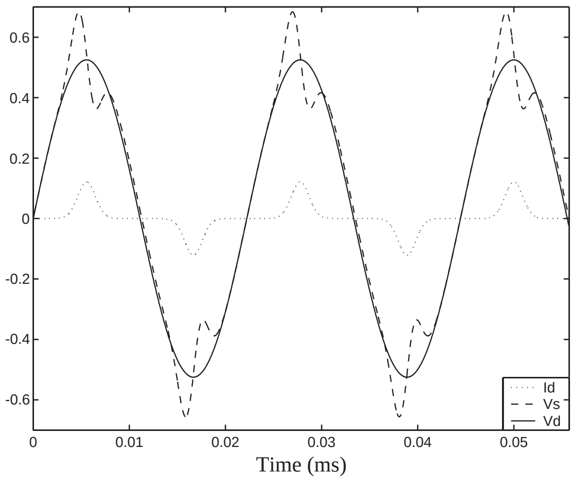

Fig. 4. Relation in time domain between main electrical components: I_D, electrical current ($\times 10^4$ A); V_D, voltage across diodes (V); and V_s, voltage across ultrasonic membrane (V).

Fig. 5. Experimental set-up for dynamic crop density measurements.

On both sides of the cart, an ultrasonic transducer is placed. One sensor is placed as sender, the other one as receiver. By this, measurements are possible in transmission and in reflectance and this with different cart speeds.

One of the problems of the use of inverters is the electromagnetic interference. The carrier frequency of the converter must be high enough to prevent low-force harmonics and subsequently, to ensure a smooth speed course of the cart. Practically, the carrier frequency must be at least 10 kHz, bringing about strong harmonics close to the working frequency of the ultrasonic transducer (40–60 kHz). For preventing strong interference and by thus aliasing effects, a second order, electronic band-pass filter is implemented before the actual signal is acquired.

As excitation signal, the standard burst can be implemented. This short signal is generated by triggering an internal electronic circuit. For measurements in transmission, a normal signal generator is used for stationary sine waves.

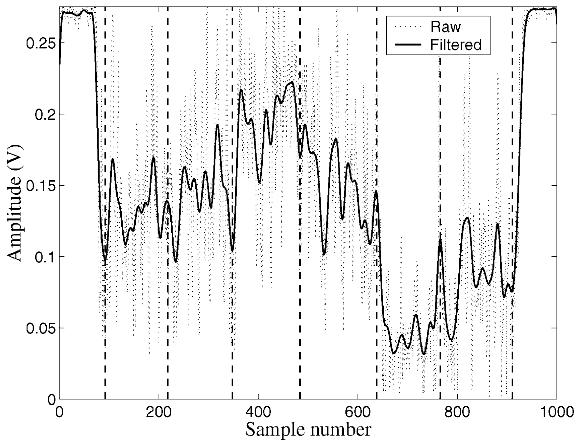

Fig. 6. Raw and filtered amplitude of signal V_s (V). Dashed lines separate the sections with stem densities of, respectively, 367, 275, 165, 367, 826 and 496 stems/m^2.

3. Results

Two types of ultrasonic measurements are carried out. First, measurements of ultrasonic, reflected waves are analyzed and subsequently, measurements in transmission are carried out.

3.1. Measurements of reflected waves

With the purpose of practical implementation, measurements on reflected ultrasonic waves are interesting. One sensor could be placed on the machine and could work both as transmitter and receiver. Since the working principle would be based on the analysis of a burst signal, the distance to the crop could be estimated as well.

The problem of reflection measurement is the physical background of the received signal. Fig. 7 exhibits four reflected waves on the same crop. The only difference is the position of the ultrasonic transducer. Between each measurement, the sensor is moved 1 cm along the crop. Although the crop density has not changed, the shape of the reflected wave is totally different. The only consistency between the four signals is the appearance of two clusters: the first one starting at about 2 ms after emission, the second one after 3 ms. These clusters correspond with, respectively, the first and second rows of wheat plants.

The non-consistency of the cluster itself is due to the spatial influence of the phase shift between each reflected burst (Fig. 8). Time signal V_s corresponding to one burst can be written as

$$V_s(t) = \sum_{i=1}^{N} a_i(l_i)u\left(t - \frac{l_i}{330}\right), \quad (3)$$

where N denotes the number of reflected signals; $a_i(l_i)$, the attenuation ratio of the ith reflected burst; l_i, the distance to the ultrasonic transducer in metres and $u(t)$, the transmitted signal. In fact, $a_i(l_i)$ depends on the orientation and the arrangement of the plants. The crop density will

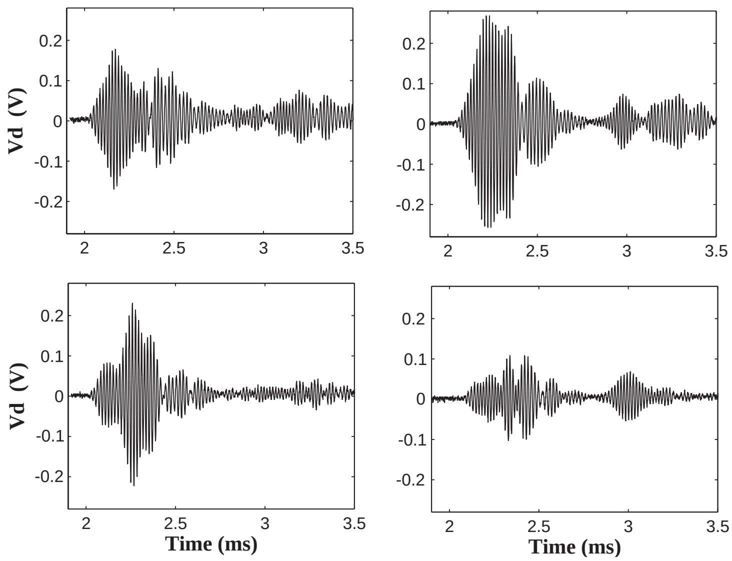

Fig. 7. Four different reflected burst signals V_D of four placements with 1 cm distance and pointed on the same crop density.

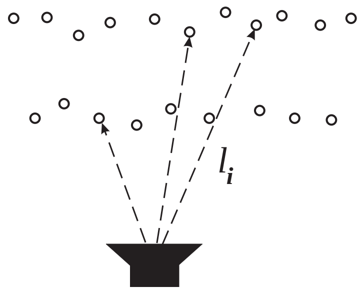

Fig. 8. Physical background of clustered signal with l_i denoting half the travel distance of one burst.

mainly have an affect on the number of reflections N and the attenuation coefficients $a_i(l_i)$. The denser the first row of crop, the more it contributes to the total reflection.

The origin of the non-predictable shape of the burst is mainly the cause of the influence of l_i on the phase. The wavelength of 55 kHz-sines is 6 mm. This implies that signals i and j with $|l_i - l_j| = 0.0015$ are in anti-phase and compensate each other. This makes it only possible to estimate the crop density if the ultrasonic beam is sufficiently narrow. This latter condition is inherently associated with a high variance crop density estimation because of the small surface. Therefore, crop density estimators based on reflection are not possible with standard signal processing techniques.

3.2. Measurements in transmission

Secondly, one ultrasonic sensor is installed as transmitter, the other one as receiver. As excitation, a sine is applied via a standard signal generator. This 5 V-signal is applied via the primary of transformer T_1 (Fig. 1). The transmitted signal is a sine wave and the parameter directly related with the crop density is the amplitude of the received wave. Again, to ensure an unbiased amplitude estimation, the implementation of Eq. (2) is necessary.

The excitation frequency is chosen corresponding with the highest repeatability of the density estimation. Different runs are performed in both directions and the similarity of the corresponding signals is compared. As result, 50 kHz gave the best result and is therefore chosen for the measurements.

The speed influence can be neglected. The physical property of the attenuation is based on the covering of surface between both sensors. The wave frequency has no influence on this process and the high frequency makes it possible to estimate the amplitude as frequently as wanted.

The distance between both sensors in this set-up is less than 1 m. The diameter of both membranes is 5 cm. By this, the measurement is based on a small surface and therefore, local density deviations will have an important impact. Fig. 6 illustrates the subsequent amplitude estimations. With the assumption of a constant cart speed, the sample number can be brought back to a spatial co-ordinate. The raw estimations (**x**) show a lot of variance. As a consequence, a non-causal filter is introduced to smooth these amplitude estimations. As a filter, a convolution with a normalized 25-points, *Hamming* window is chosen. Each filtered estimation of the local density is partially based on the neighbouring, resulting in a smoothed density signal.

The amplitude estimation is based on short, equidistant strokes of a signal. The previous amplitude estimation is as much related to the following estimation which makes the appropriate filter non-causal and symmetric. The solid line of Fig. 6 illustrates the result. Each section is planted in its own wooden box. This constructions brings about plant stems at the boundary of each sections which are directed towards each other. This effect is visible by large tips and dips in the transmission signal.

Once a parameter, closely related with the crop density is found, a first calibration curve is set up. This curve is based on an average across each crop density. Both ends of the signal give information about the offset and provide a possibility to remove a linear trend of the influence of heat on the characteristics of the consisting components (resistor and diodes).

Fig. 9 shows the resulting calibration curve between crop density and the amplitude of voltage V_s. Each point corresponds with an averaged amplitude value for one crop density during one run. Experiments showed that the variance between subsequent runs is mainly due to the influence of working temperature on the electronic components. This sensor is not designed to generate stationary ultrasonic waves and therefore, a new thermodynamic calculation of the consisting components must be carried out before this method can be implemented for longtime applications. The low amplitude values of Fig. 9 indicates that the non-linearity can be described by the first part of Eq. (2).

The trend line of Fig. 9 is given by a simple exponential curve:

$$V_s = 0.2719 \exp^{-0.0021D}, \tag{4}$$

where D denotes the crop density of wheat plants in stems/m^2.

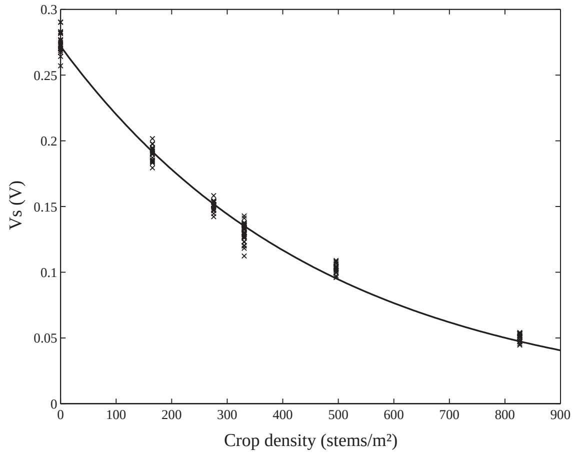

Fig. 9. Calibration curve relating crop density of wheat plants (stems/m^2) to V_s (V).

4. Conclusions

In this study, a standard ultrasonic distance sensor is used to estimate the crop density of wheat plants. An appropriate signal V_D is measured, closely related with the ultrasonic vibration of the membrane Us.

A 10 m experimental set-up is made for dynamic measurements. Two arrangements are tested:

- First, the difficulty of ultrasonic reflection measurements has been shown. Due to the significant influence of the plant arrangement on the measured signals, standard techniques do not satisfy the requirements. Advanced techniques must be introduced to get useful results.
- As second experiment, dynamic ultrasonic crop density measurements are carried out in transmission. Although this set-up is not as practical as for reflection, first promising results are achieved.

The impact of a varying environmental moisture content is negligible for both experimental set-ups because of the small distance between the transmitting and receiving membranes. The influence of a changing moisture content of the crop does not play a role either since the transmission of the ultrasonic waves through the stems can be neglected.

Acknowledgements

The authors gratefully acknowledge the Instituut voor Wetenschappelijk Technologisch onderzoek (IWT) for the financial support through doctoral grant No. 003249. This study has been made possible through cooperation of New Holland, Belgium.

References

[1] P.A. Barbieri, H.R. Sainz Rozas, F.H. Andrade, H.E. Echeverria, Row spacing effects on different levels of nitrogen availability in maize, *Agronomy Journal* 92 (2000) 283–288.

[2] T.L. Henderson, B.L. Johnson, A.A. Schneiter, Row spacing, plant population, and cultivar effects on grain amaranth in the northern great plains, *Agronomy Journal* 92 (2000) 329–336.

[3] P.D. Adams, D.B. Weaver, Brachytic stem trait, row spacing and plant population effects on soybean yield, *Crop Science* 38 (1998) 750–755.

[4] J.C. Taylor, G.A. Wood, G. Thomas, Mapping yield potential with remote sensing, in: J.V. Stafford (Ed.), *Proceedings of the First European Conference on Precision Agriculture*, SCI, London, 1997, pp. 713–720.

[5] J.C. Taylor, G.A. Wood, J.P. Welsh, S. Knight, Exploring management strategies for precision farming of cereals assisted by remote sensing, in: *Aspects of Applied Biology*, *Vol. 60*, *Remote Sensing in Agriculture*, Association of Applied Biologists, Royal Agricultural College, Cirencester, 2000, pp. 53–60.

[6] R.K. Taylor, M.L. Stone, H.W. Downs, Mapping yield potential with remote sensing, ASAE Paper No. 86-1619, 1986.

[7] B. Missotten, Measurement Systems for the Mapping and the Evaluation of Crop Production Performance, Ph.D. Thesis, Department of Agro-Engineering and Economics, Katholieke Universiteit Leuven, 1998.

[8] D. Ehlert, H. Smith, Site-specific measuring of biomass in standing plant populations, *Landtechnik* 51 (2) (1996) 86–87.

[9] J. De Clippel, Ontwikkeling van een standdichtheidssensor voor graangewassen [Development of a crop density sensor for cereal crops], Master's Thesis, Katholieke Universiteit Leuven, 2000.

[10] R. Vansichen, J. De Baerdemaeker, Measuring the actual cutting width of a combine by means of an ultrasonic distance sensor, in: *Trends in Agricultural Engineering*, Prague, 15–18 September, 1992, pp. 615–621.

[11] J.A. Nelder, R. Lead, A simplex method for function minimization, *Computer Journal* 7 (1965) 308–313.